Study of inclusive single-jet production in the framework of k_t-factorization unintegrated parton distributions

R. Aminzadeh Nik, M. Modarres,[*] and M. R. Masouminia
Department of Physics, University of Tehran, 1439955961 Tehran, Iran

(Received 7 February 2018; published 29 May 2018)

The present work is intended to study the double-differential cross section of the inclusive single-jet production as the functions of the transverse momentum and the rapidity of the jet in the high-energy hadron-hadron collisions. The angular-ordering-constraint k_t-factorization framework is used to calculate the above cross section that is available experimentally. The conditions are taken in accordance with the LHC experiments. The results are compared and analyzed using the existing CMS LHC data. The scheme-dependent unintegrated parton distribution functions (UPDF) of Kimber-Martin-Ryskin (KMR) and Martin-Ryskin-Watt (MRW) in the leading-order and the next-to-leading order (NLO) are used to predict the input partonic UPDF. The utilized phenomenological frameworks prove to be relatively successful in generating satisfactory results compared to the different experiment data, such as CMS (8 and 13 TeV). Extensive discussions and comparisons are made regarding the behavior of the contributing partonic subprocesses. Finally, it is shown that the application of the KMR UPDF to the single-jet differential cross sections have better agreement with the CMS data; on the other hand, they are very similar to those of NLO-MRW.

DOI: 10.1103/PhysRevD.97.096012

I. INTRODUCTION

Measurement of the jet production cross sections in the proton-proton collisions is a useful and vital test of QCD. These processes are visible in most of the parton-parton high-energy scatterings in the hadron colliders. The study of jet production events in general makes it possible to obtain valuable information regarding the functionality of parton distribution functions (PDF) [1], as well as to provide a probe of the strong coupling constant, α_s, up to the highest energy scales that can be attained in the collider experiments [2,3]. Additionally, the single-jet production events are a direct window to observing the true nature of partonic interactions. One of the most important of these processes is the inclusive jet production. These measurements usually are based on probing the differential cross section of inclusive single-jet production as a function of transverse momentum in the various regions of the absolute rapidity, y, of the jets.

The analysis of the double-differential inclusive single-jet data is performed at the same center-of-mass energy by many experimental collaborations. The LHC, the ATLAS, and the CMS Collaborations measured the double-differential cross section of the inclusive single-jet production events at 2.76 and 7 TeV [4–9] (several to a few years ago). Similar measurements were taken at the Tevatron by the D0 and the CDF Collaborations at 1.96 TeV [10–12] in the same period.

In the recent measurements, the single-jet double-differential cross section is investigated at the high center-of-mass energies at the LHC. The CMS Collaboration tried to extend their previous investigations by increasing the center-of-mass energy to 8 and 13 TeV [3,13], respectively.

Today, many of the high energy physics laboratories use PDFs to describe and analyze their extracted data from the deep inelastic QCD collisions. These scale-dependent functions are the solutions of the Dokshitzer-Gribov-Lipatov-Altarelli-Parisi (DGLAP) evolution equations [14–17], enriched by the extended QCD supplements such as the parton showers and the fragmentation effects. The DGLAP evolution equation, however, is based on the strong ordering assumption, which systematically neglects the transverse momentum of the emitted partons along the evolution ladder. It has repeatedly been hinted that undermining the contributions coming from the transverse momentum of the partons may severely harm the precision of the calculations, especially in the high-energy processes in the small-x region; see, for example, Refs. [18–22]. This signaled the necessity of introducing some transverse momentum-dependent (TMD) PDF, e.g., through the Catani-Ciafaloni-Fiorani-Marchesini (CCFM) [23–29] of Balitsky-Fadin-Kuraev-Lipatov (BFKL) [30–34] evolution equations.

Solving the CCFM and the BFKL equations is typically difficult and makes the calculation procedures very complicated. On the other hand, the main feature of the CCFM equation, i.e., the angular ordering constraint, can be

[*]Corresponding author.
mmodares@ut.ac.ir

exclusively used for the gluon evolution. To overcome these obstacles, Martin *et al.* introduced the k_t-factorization framework and developed the Kimber-Martin-Ryskin (KMR) and the Martin-Ryskin-Watt (MRW) approaches [35,36], both of which are constructed from the leading order (LO) DGLAP evolution equations and modified with the different visualizations of the angular ordering constraint. The frameworks of KMR and MRW in the LO and the next-to-leading order (NLO) have been investigated intensely in recent years; see Refs. [37–48].

In the present paper, we intend to numerically calculate the rate of production of single jets, using a simplistic LO set of matrix elements and the unintegrated parton distribution functions (UPDF) of the k_t factorization, i.e., the KMR [35] and the MRW UPDF in the LO and NLO orders [36]. To this end, we make use of a hybrid partonic

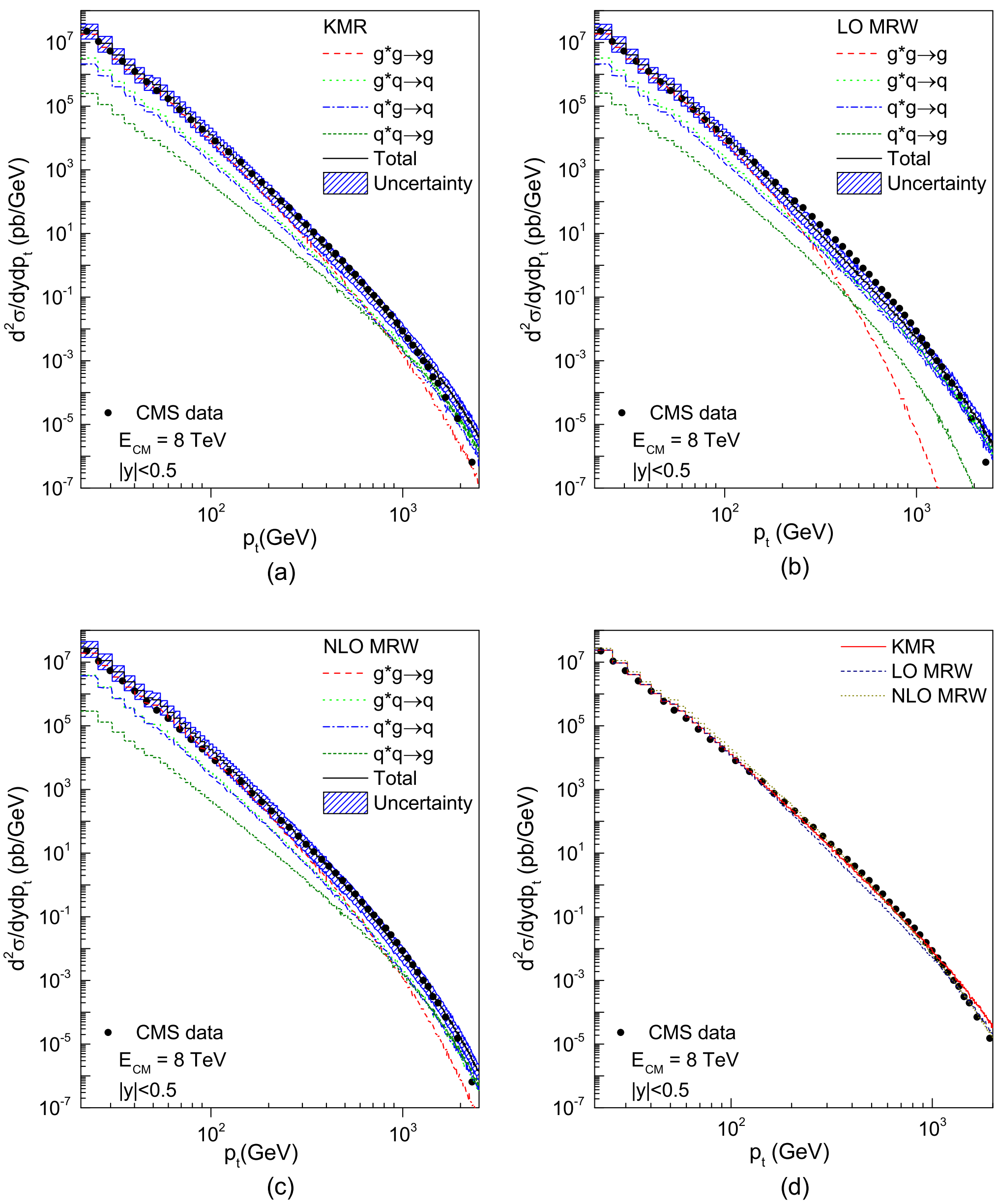

FIG. 1. The double-differential cross section for the production of a single jet as a function of the transverse momentum of the resulting jet. The corresponding numerical calculations are carried out within the given rapidity boundaries (see the legends of the plots), utilizing the UPDF of KMR, LO and NLO MRW for $E_{\mathrm{CM}} = 8$ TeV. The results are shown in panels (a), (b), and (c), respectively. These panels also outline the contributions of the involving partonic subprocesses. The uncertainty regions are designated via manipulating the hard scale of the processes by a factor of 2. Panel (d) presents a comparison between these results against each other and against the experimental data of the CMS Collaboration [3].

framework (i.e., we assume one of the incoming partons in the collinear and the other in the k_t-factorization framework) [47,49,50]. Afterward, we will compare our results with the existing experimental data from the CMS Collaboration [3,13].

Throughout this work, we follow the footsteps of Kutak *et al.* [49], where a similar hybrid framework was used to calculate the production rates of single jets in the forward rapidity sector. Therefore in their work, in order to describe the incoming off-shell partons, a number of different TMD PDF frameworks were used, i.e., the Kutak-Sapeta (KS)-nonlinear [51–54], the KS-linear [53], and the KS hard-scale linear and nonlinear frameworks [55], as well as the double log coherence (DLC)2016 formalism [56]. However, contrary to the case of Ref. [49], we have extended the range of the rapidity of the produced jets to a wider spectrum, i.e., $0 < |y| < 4.7$, to test and analyze the potential of the hybrid framework in predicting the results, outside the forward sector.

In the following, the theoretical framework of the single inclusive jet production events at the LHC and a brief introduction to the KMR, the LO MRW, and the NLO MRW prescriptions are presented in Sec. II. Section III is devoted to our results and discussions. Finally a short conclusion is given in Sec. IV.

II. THE THEORETICAL FRAMEWORK

The inclusive single-jet production events are rather clear processes since the fragmentation does not have essential contributions in them. Therefore, we can investigate the partonic structure of the proton at each energy while

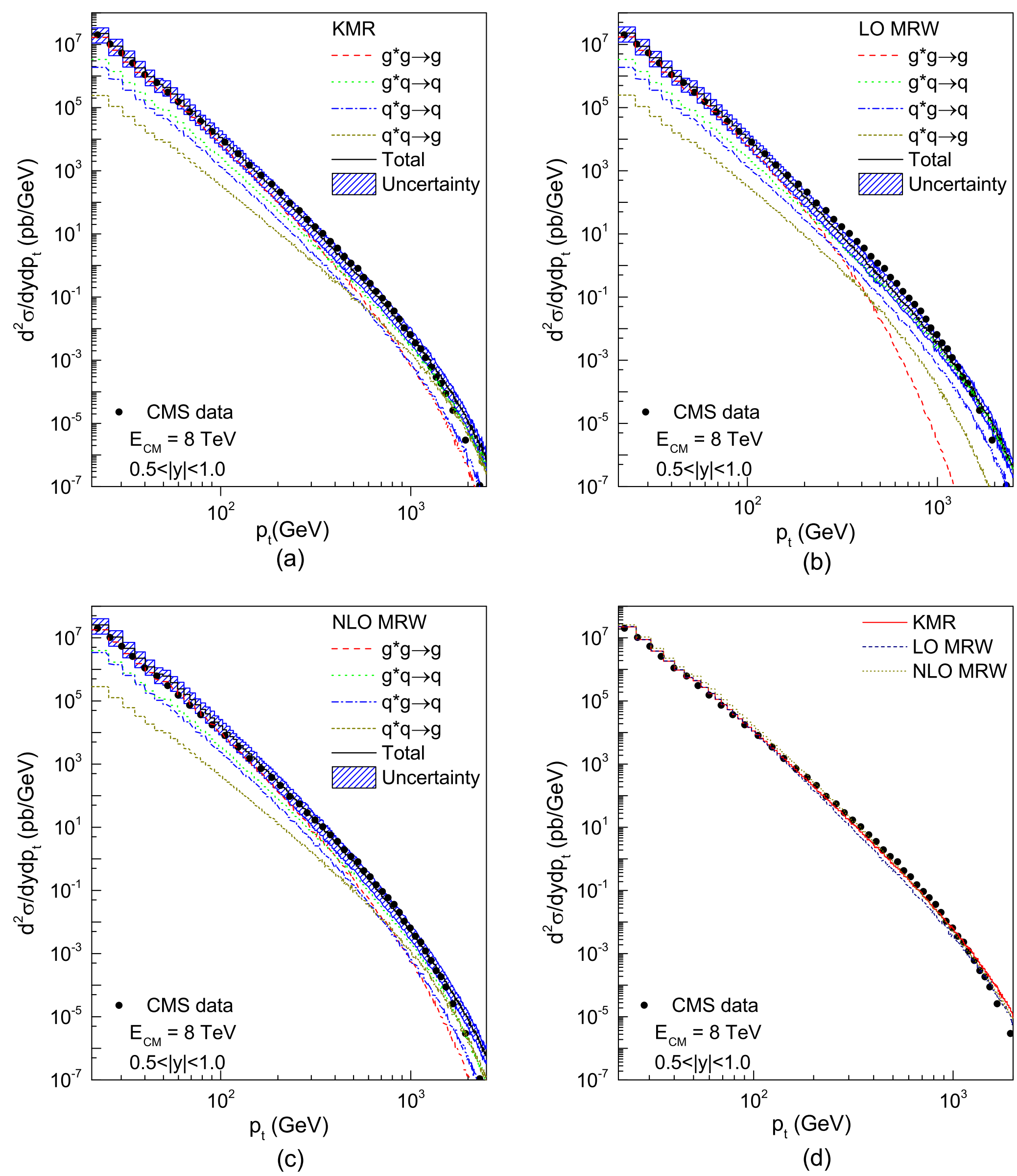

FIG. 2. As Fig. 1 but for a different rapidity region.

applying the necessary constraints on the experiments. Furthermore, the higher-order perturbative quantum-chrome-daynamics (pQCD) does not considerably affect the results. In general, the inclusive single-jet production in the hadron-hadron colliders can be described as follows:

$$A + B \to a + b \to \text{jet} + X,$$

where a and b are the partons that are emitted by the incoming hadrons (A and B) and X is the usual reminder. In this paper, a set of LO $2 \to 1$ Feynman diagrams are used to represent the partonic sector of the above process. These are contrived as the following three partonic subprocesses:

$$g + g \to g, \qquad q + g \to q, \qquad q + q \to g. \qquad (1)$$

To perform the necessary calculations, we should determine the kinematics of these processes. Therefore, we chose the 4-momentum vectors of the colliding protons as

$$P_1 = \frac{\sqrt{s}}{2}(1,0,0,1), \qquad P_2 = \frac{\sqrt{s}}{2}(1,0,0,-1),$$

where s is the center-of-mass energy. By using the Sudokov decomposition,

$$\mathbf{k}_i = x_i \mathbf{P}_i + \mathbf{k}_{i,t}, \qquad (2)$$

the 4-momenta of the ith parton can be obtained as the functions of the transverse momenta, $k_{i,t}$, and the

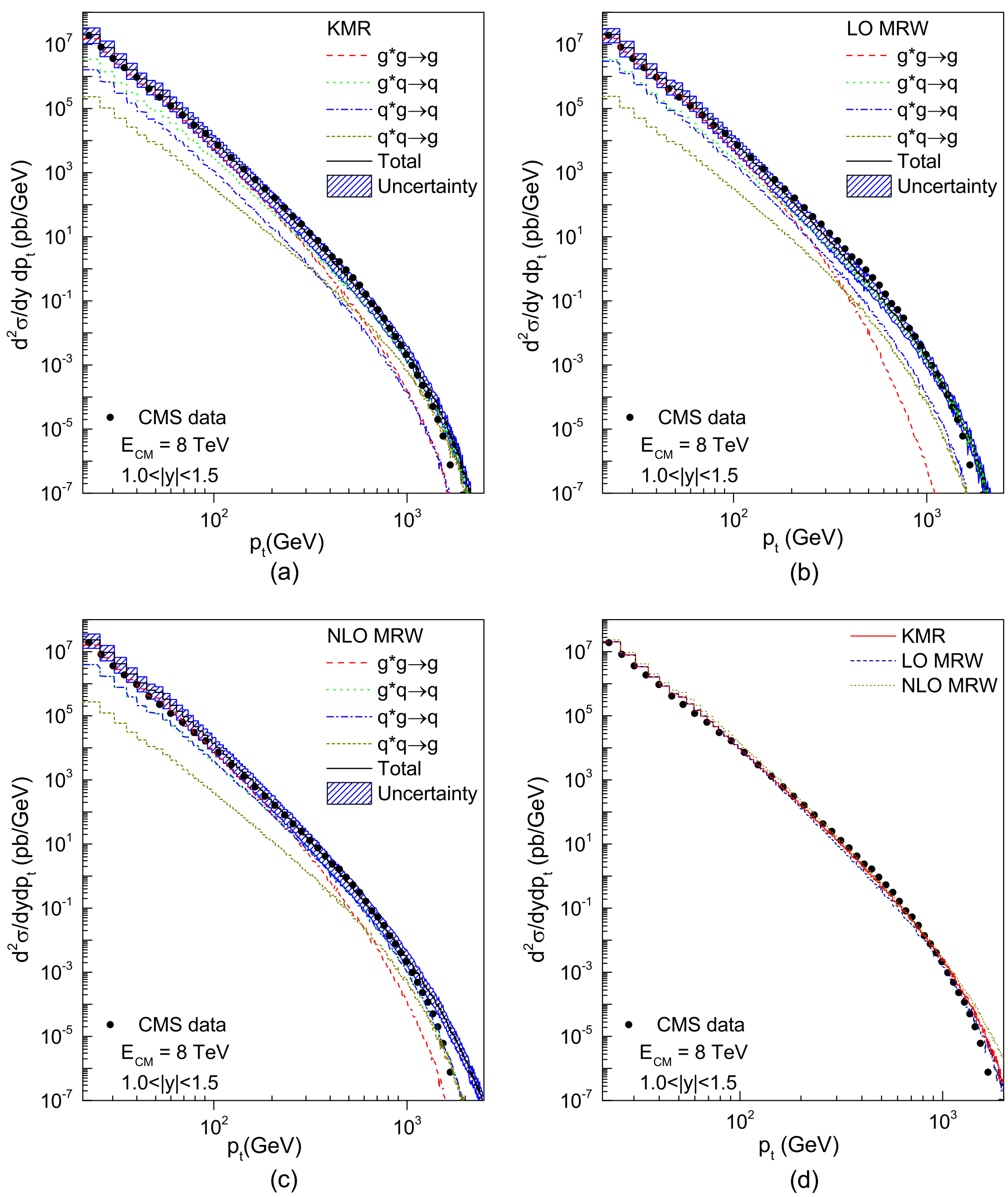

FIG. 3. As Fig. 1 but for a different rapidity region.

longitudinal fraction of the momentum, x_i. These are considered as inherited parameters for a given parton. The above momenta can be described as

$$k^\mu = \left(\sqrt{\frac{M^2 + p_t{}^2}{2}} e^y, \sqrt{\frac{M^2 + p_t{}^2}{2}} e^{-y}, P_t\right),$$

where p_t and y are the transfer momentum and the rapidity of the outgoing jet, respectively. Considering the subprocesses of Eq. (2) and the conservation law of energy momentum, the relation among the Bjorken variable (x), the transfer momentum (p_t^{jet}), and the rapidity (y^{jet}) is obtained as

$$x_2 = \frac{1}{\sqrt{s}} p_t^{\mathrm{jet}} e^{y_{\mathrm{jet}}}, \qquad x_1 = \frac{1}{\sqrt{s}} p_t^{\mathrm{jet}} e^{-y_{\mathrm{jet}}}. \tag{3}$$

We make use of the usual framework in our calculation of the inclusive single-jet production (i.e., the hybrid framework) which is introduced in Ref. [49]. This framework sets a particular distinction between the input partons, directly related to their transverse momenta. By this sense, all the input transverse momentum is considered to be carried by one of the incoming partons, say the first, while the second parton has no transverse momentum. Hence, the second parton can be considered to be in the collinear framework, and its behavior can be described directly as the solutions of the LO DGLAP evolution equation. Consequently, we chose to rewrite the relations (2) as follows:

$$g^* + g \to g, \tag{4}$$

$$q^* + g \to q, \tag{5}$$

$$g^* + q \to q, \tag{6}$$

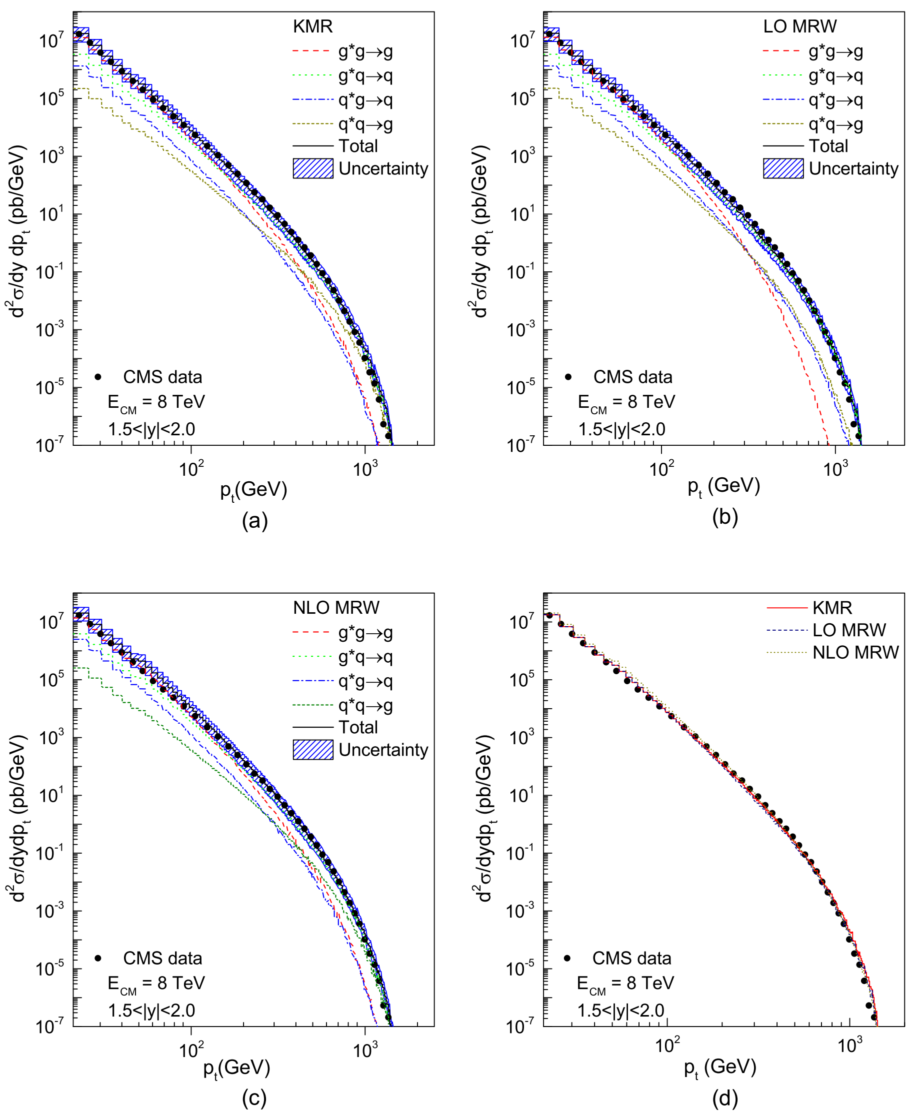

FIG. 4. As Fig. 1 but for a different rapidity region.

$$q^{*} + q \to g. \tag{7}$$

Here the parton with the star sign carries transverse momentum and should be described by the corresponding UPDF of the k_t factorization. The result is the differential cross section of inclusive single-jet production at the hybrid phase space [49,57], which reads as

$$d^2\sigma/dp_t^{\rm jet}dy_{\rm jet} = \sum_{a,b,c} \frac{\pi p_t^{\rm jet}}{2(x_1x_2s)^2}|\mathcal{M}_{a^*b\to c}|^2 \times \mathcal{F}_a(x_1, p_{t,\rm jet}^2, \mu^2)x_2 f_b(x_2, \mu^2), \tag{8}$$

where $\mathcal{F}_a(x_1, p_{t,\rm jet}^2, \mu^2)$ is the UPDF that depends on the three parameters (i.e., x_1, $p_{t,\rm jet}^2$, and μ^2).

The UPDF can be directly obtained from the PDF, using different prescriptions. In this paper, we use three approaches, namely KMR [35], LO-MRW, and NLO-MRW [36], to generate the UPDF from the PDF to insert in Eq. (8). At the high center-of-mass energy, in the small-x region and high rapidity y regions, the transverse momentum, k_t, of the incoming partons are expected to become more important, where the incoming partons are treated as the off-shell particles [18,45,58]. So, the UPDF $[\mathcal{F}(x_1, p_{t,jet}^2, \mu^2)]$ and the PDF $[f_a(x_2, \mu^2)]$ are used in

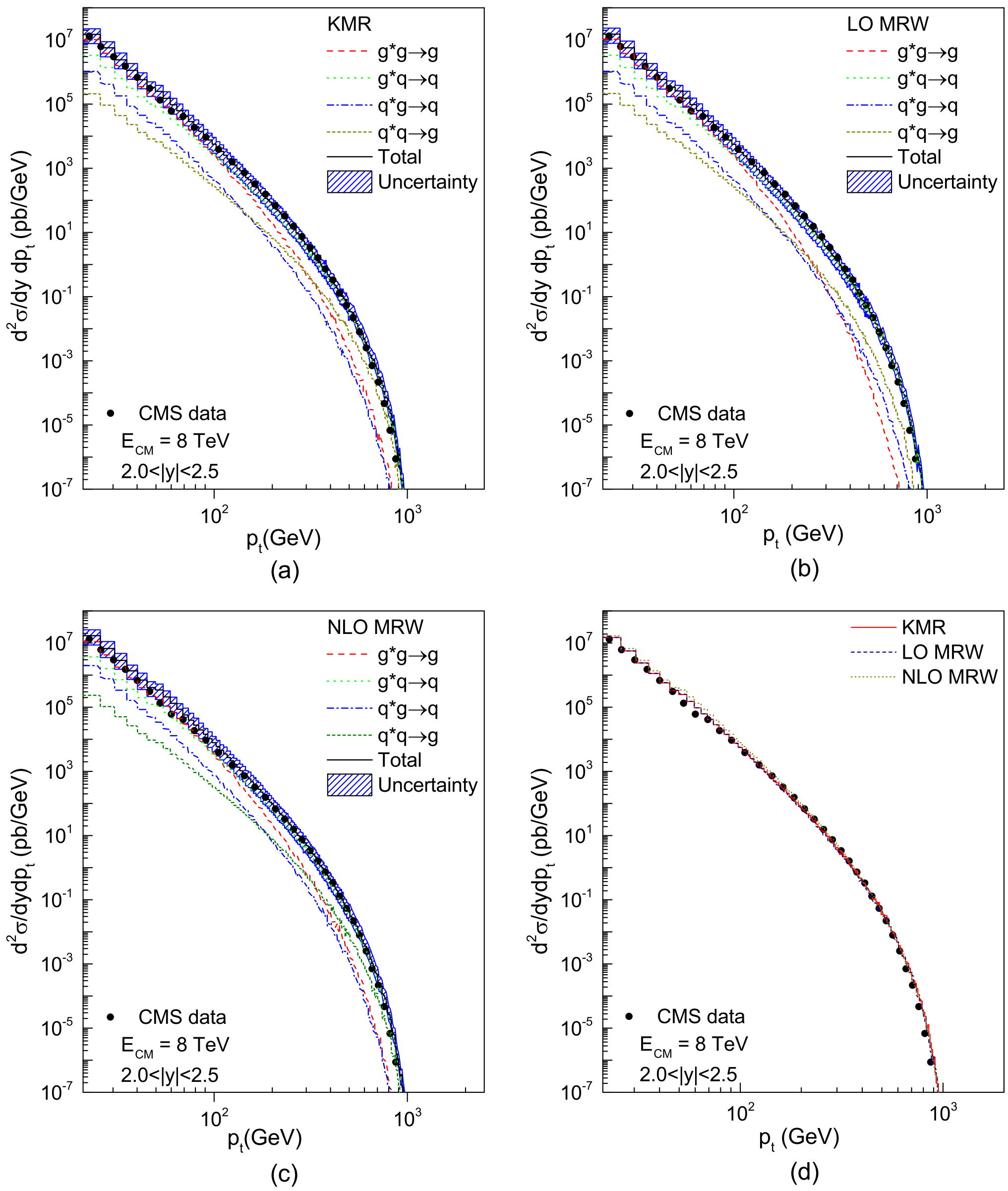

FIG. 5. As Fig. 1 but for a different rapidity region.

Eq. (8) for incoming partons with x_1 and x_2 Bjorken variables, respectively.

The KMR UPDF is built so that the parton evolves from starting parametrization up to the scale k_t according to the DGLAP evolution equation [35]. In this formalism partons evolve in the single evolution ladder (carrying only the k_t^2 dependency) and get convoluted with the second scale (μ^2) at the hard process. KMR assume that the k_t depends on the scale μ^2, without any real emission and by summing over the virtual contributions via imposing the Sudokov form factor [$T_a(k_t^2, \mu^2)$]. So, the general form of the KMR UPDF is

$$f_a(x, k_t^2, \mu^2) = T_a(k_t^2, \mu^2) \sum_{b=q,g} \left[\frac{\alpha_S(k_t^2)}{2\pi} \int_x^{1-\Delta} dz P_{ab}^{(\mathrm{LO})}(z) b\left(\frac{x}{z}, k_t^2\right) \right], \tag{9}$$

where $T_a(k_t^2, \mu^2)$ are

$$T_a(k_t^2, \mu^2) = \exp\left(-\int_{k_t^2}^{\mu^2} \frac{\alpha_S(k^2)}{2\pi} \frac{dk^2}{k^2} \sum_{b=q,g} \int_0^{1-\Delta} dz' P_{ab}^{(\mathrm{LO})}(z') \right). \tag{10}$$

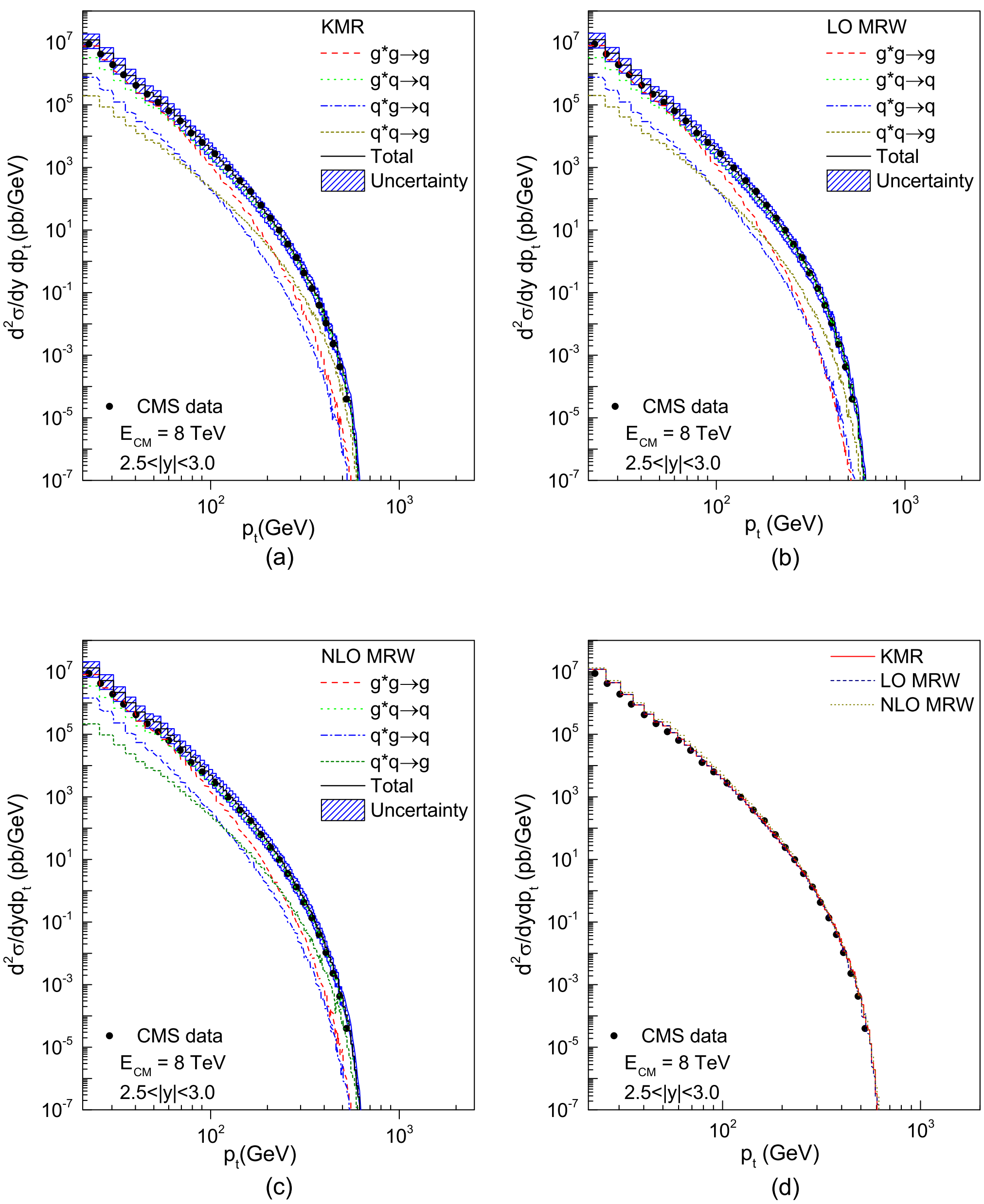

FIG. 6. As Fig. 1 but for a different rapidity region.

T_a are considered to be unity for $k_t > \mu.\Delta$ in the above equation is proposed to prevent the soft gluon singularity, but this constraint is imposed on the quark radiations too. In order to determine Δ, the angular ordering constraint is imposed. Angular ordering originates from the color coherence effects of the gluon radiations [35]. So Δ is

$$\Delta = \frac{k_t}{\mu + k_t}.$$

The $P_{ab}^{(\mathrm{LO})}(z)$ are the familiar LO splitting functions [59]. We remark that recently in Ref. [60], some ambiguities about the different choices of the cutoff, Δ, in the KMR approach [35,61] were discussed. Furthermore, it was shown that [60] the computed UPDF is particularly the same, if one chooses the ordinary or cutoff dependent PDF in the calculations. Hence the KMR UPDF should be evaluated directly from the global fitted PDF, similar to the procedures performed in the present work.

The LO-MRW UPDF is similar to the KMR scheme, but only when the angular ordering constraint is correctly imposed on the on-shell radiated gluons, i.e., the diagonal splitting functions $P_{qq}(z)$ and $P_{gg}(z)$ [36]. So, the LO-MRW prescription is written as

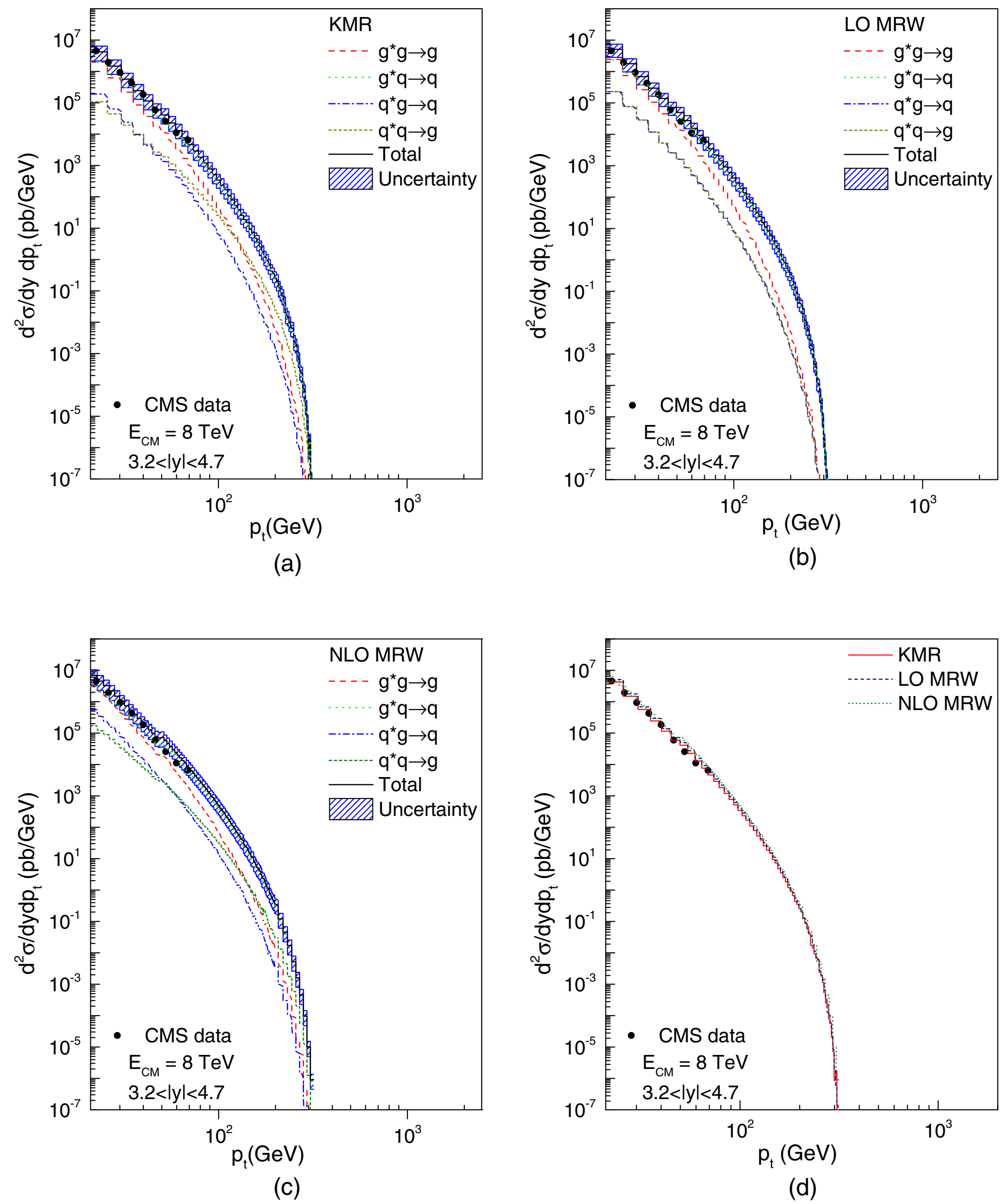

FIG. 7. As Fig. 1 but for a different rapidity region.

$$f_q^{\mathrm{LO}}(x,k_t^2,\mu^2) = T_q(k_t^2,\mu^2)\frac{\alpha_S(k_t^2)}{2\pi}\int_x^1 dz\left[P_{qq}^{(\mathrm{LO})}(z)\frac{x}{z}q\left(\frac{x}{z},k_t^2\right)\times\Theta\left(\frac{\mu}{\mu+k_t}-z\right)+P_{qg}^{(\mathrm{LO})}(z)\frac{x}{z}g\left(\frac{x}{z},k_t^2\right)\right], \quad (11)$$

with

$$T_q(k_t^2,\mu^2) = \exp\left(-\int_{k_t^2}^{\mu^2}\frac{\alpha_S(k^2)}{2\pi}\frac{dk^2}{k^2}\int_0^{z_{\max}}dz' P_{qq}^{(\mathrm{LO})}(z')\right), \quad (12)$$

for the quarks, and

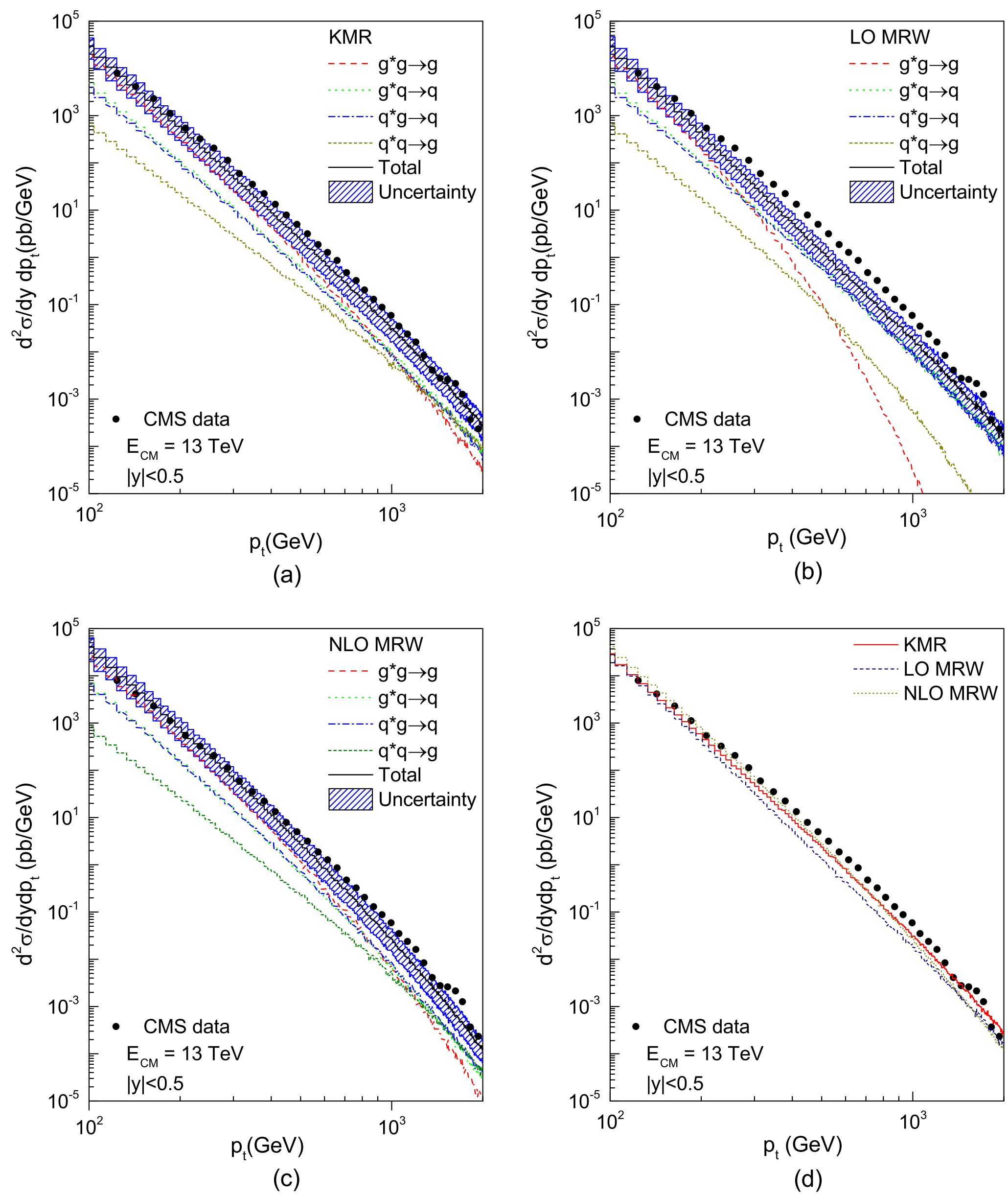

FIG. 8. The double-differential cross section for the production of a single jet as a function of the transverse momentum of the resulting jet. The corresponding numerical calculations are carried out within the given rapidity boundaries (see the legends of the plots), utilizing the UPDF of KMR, LO and NLO MRW for $E_{\mathrm{CM}} = 13$ TeV. The results are shown in panels (a), (b), and (c), respectively. These panels also outline the contributions of the involving partonic subprocesses. The uncertainty regions are designated via manipulating the hard scale of the processes by a factor of 2. Panel (d) presents a comparison between these results against each other and against the experimental data of the CMS Collaboration [13].

$$f_g^{\rm LO}(x,k_t^2,\mu^2) = T_g(k_t^2,\mu^2)\frac{\alpha_S(k_t^2)}{2\pi}\int_x^1 dz\left[P_{gq}^{(\rm LO)}(z)\sum_q \frac{x}{z}q\left(\frac{x}{z},k_t^2\right) + P_{gg}^{(\rm LO)}(z)\frac{x}{z}g\left(\frac{x}{z},k_t^2\right)\Theta\left(\frac{\mu}{\mu+k_t}-z\right)\right], \quad (13)$$

with

$$T_g(k_t^2,\mu^2) = \exp\left(-\int_{k_t^2}^{\mu^2}\frac{\alpha_S(k^2)}{2\pi}\frac{dk^2}{k^2}\left[\int_{z_{\rm min}}^{z_{\rm max}} dz' z' P_{qq}^{(\rm LO)}(z') + n_f\int_0^1 dz' P_{qg}^{(\rm LO)}(z')\right]\right), \quad (14)$$

for the gluons. In Eqs. (12) and (14), $z_{\rm max}$ is defined as $z_{\rm max} = 1 - z_{\rm min} = \mu/(\mu + k_t)$ [20]. Martin, Ryskin, and Watt [36] proposed a method for the promotion of the LO-MRW to the NLO-MRW case. This method is based on the DGLAP evolution equation, utilizing the NLO PDF and the corresponding splitting functions [36]. The general form of the NLO-MRW UPDF is

$$f_a^{\rm NLO}(x,k_t^2,\mu^2) = \int_x^1 dz T_a\left(k^2 = \frac{k_t^2}{(1-z)},\mu^2\right)\frac{\alpha_S(k^2)}{2\pi}\sum_{b=q,g}\tilde{P}_{ab}^{(\rm LO+NLO)}(z) \times b^{\rm NLO}\left(\frac{x}{z},k^2\right)\Theta\left(1-z-\frac{k_t^2}{\mu^2}\right), \quad (15)$$

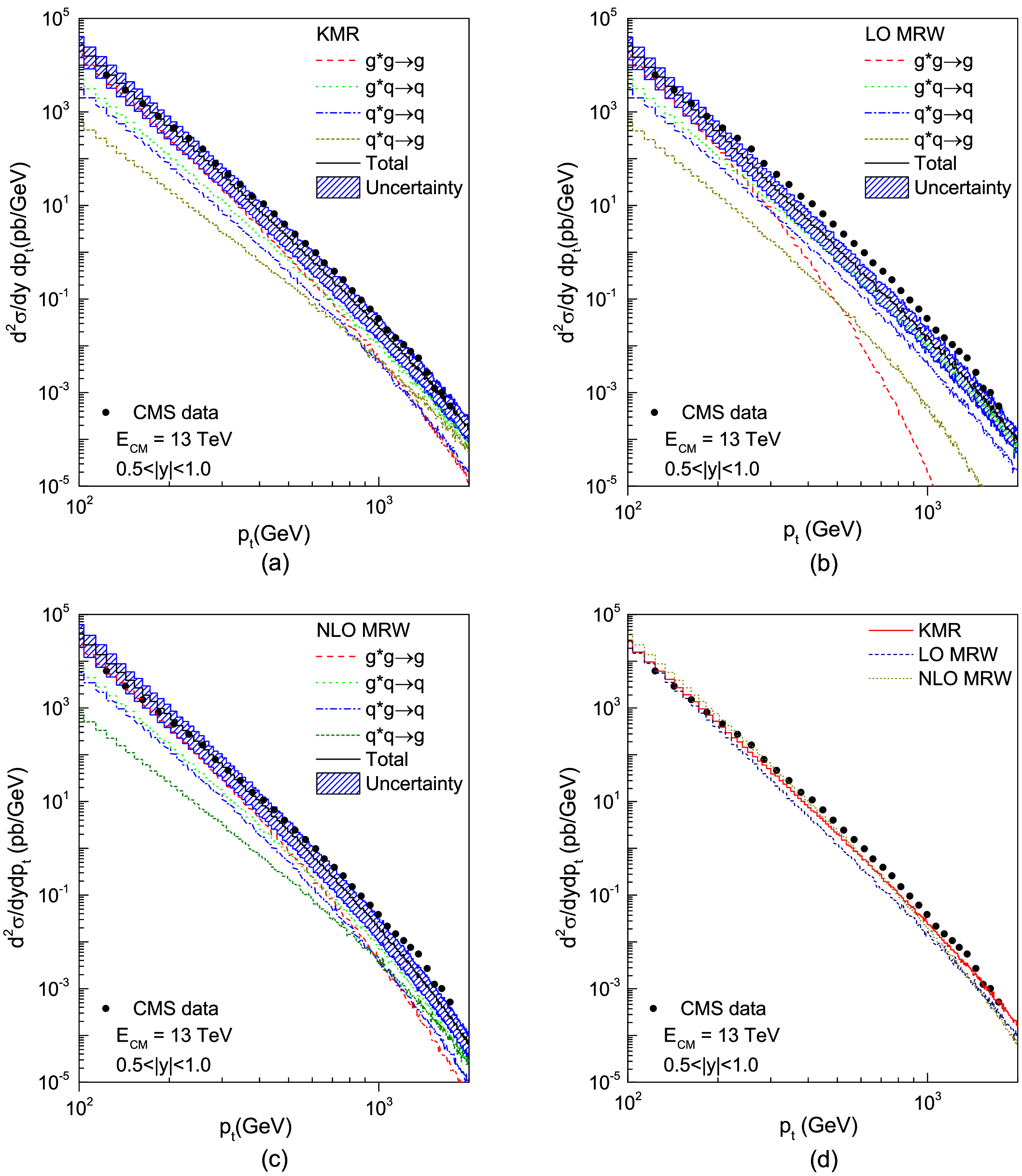

FIG. 9. As Fig. 8 but for a different rapidity region.

with the "extended" NLO splitting functions, $\tilde{P}_{ab}^{(i)}(z)$, being defined as

$$\tilde{P}_{ab}^{(\mathrm{LO+NLO})}(z) = \tilde{P}_{ab}^{(\mathrm{LO})}(z) + \frac{\alpha_S}{2\pi}\tilde{P}_{ab}^{(\mathrm{NLO})}(z), \tag{16}$$

and

$$\tilde{P}_{ab}^{(i)}(z) = P_{ab}^{i}(z) - \Theta(z-(1-\Delta))\delta_{ab}F_{ab}^{i}P_{ab}(z), \tag{17}$$

where $i = 0$ and 1 stand for the LO and the NLO, respectively. Also the angular ordering constraint is defined via the $\Theta(z-(1-\Delta))$ constraint where Δ can be defined as [36]

$$\Delta = \frac{k\sqrt{1-z}}{k\sqrt{1-z}+\mu}.$$

Finally, the Sudakov form factors in the NLO-MRW are defined as

$$T_q(k^2,\mu^2) = \exp\left(-\int_{k^2}^{\mu^2}\frac{\alpha_S(q^2)}{2\pi}\frac{dq^2}{q^2} \times \int_0^1 dz'z'\left[\tilde{P}_{qq}^{(0+1)}(z') + \tilde{P}_{gq}^{(0+1)}(z')\right]\right), \tag{18}$$

for the quarks,

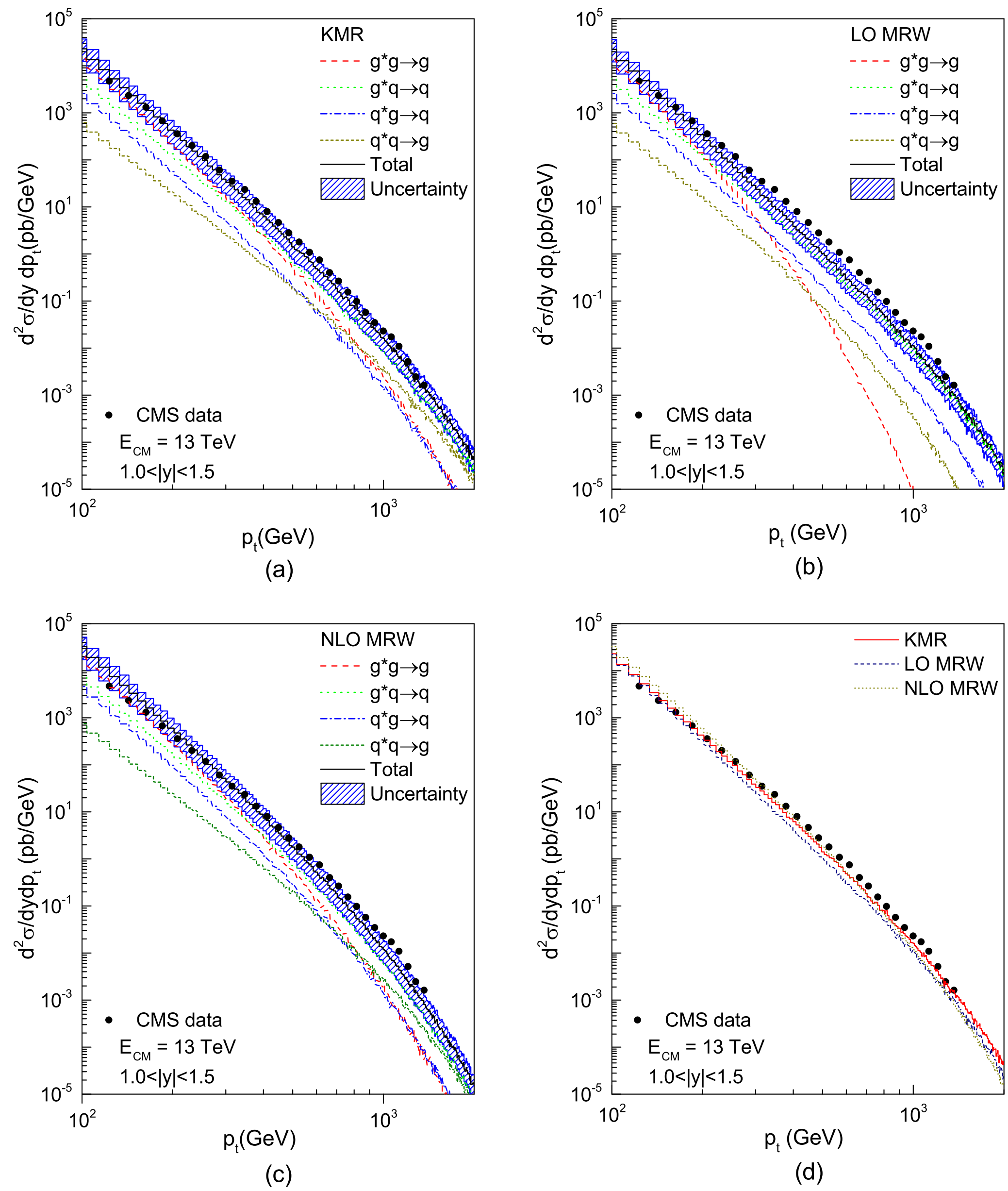

FIG. 10. As Fig. 8 but for a different rapidity region.

$$T_g(k^2,\mu^2) = \exp\left(-\int_{k^2}^{\mu^2} \frac{\alpha_S(q^2)}{2\pi}\frac{dq^2}{q^2} \times \int_0^1 dz' z' \left[\tilde{P}_{gg}^{(0+1)}(z') + 2n_f \tilde{P}_{qg}^{(0+1)}(z')\right]\right), \quad (19)$$

and for the gluons.

To calculate the double differential cross section of the single-jet production in Eq. (8), the matrix element squared ($|\mathcal{M}|^2$) of subprocesses must be calculated. By considering that the incoming partons are off shell, the matrix element for the subprocesses, which are introduced in Eqs. (4) to (7), can be written as [49]

$$|\mathcal{M}_{g^*g\to g}|^2 = 4g_s^2 \frac{C_A}{N_c^2-1}\frac{(k.q)^2}{k_t^2},$$

$$|\mathcal{M}_{g^*q\to q}|^2 = 4g_s^2 \frac{C_f}{N_c^2-1}\frac{(k.q)^2}{k_t^2},$$

$$|\mathcal{M}_{q^*g\to q}|^2 = g_s^2 \frac{C_f}{N_c^2-1}(k.q),$$

$$|\mathcal{M}_{q^*q\to g}|^2 = g_s^2 \frac{C_f}{N_c}(k.q).$$

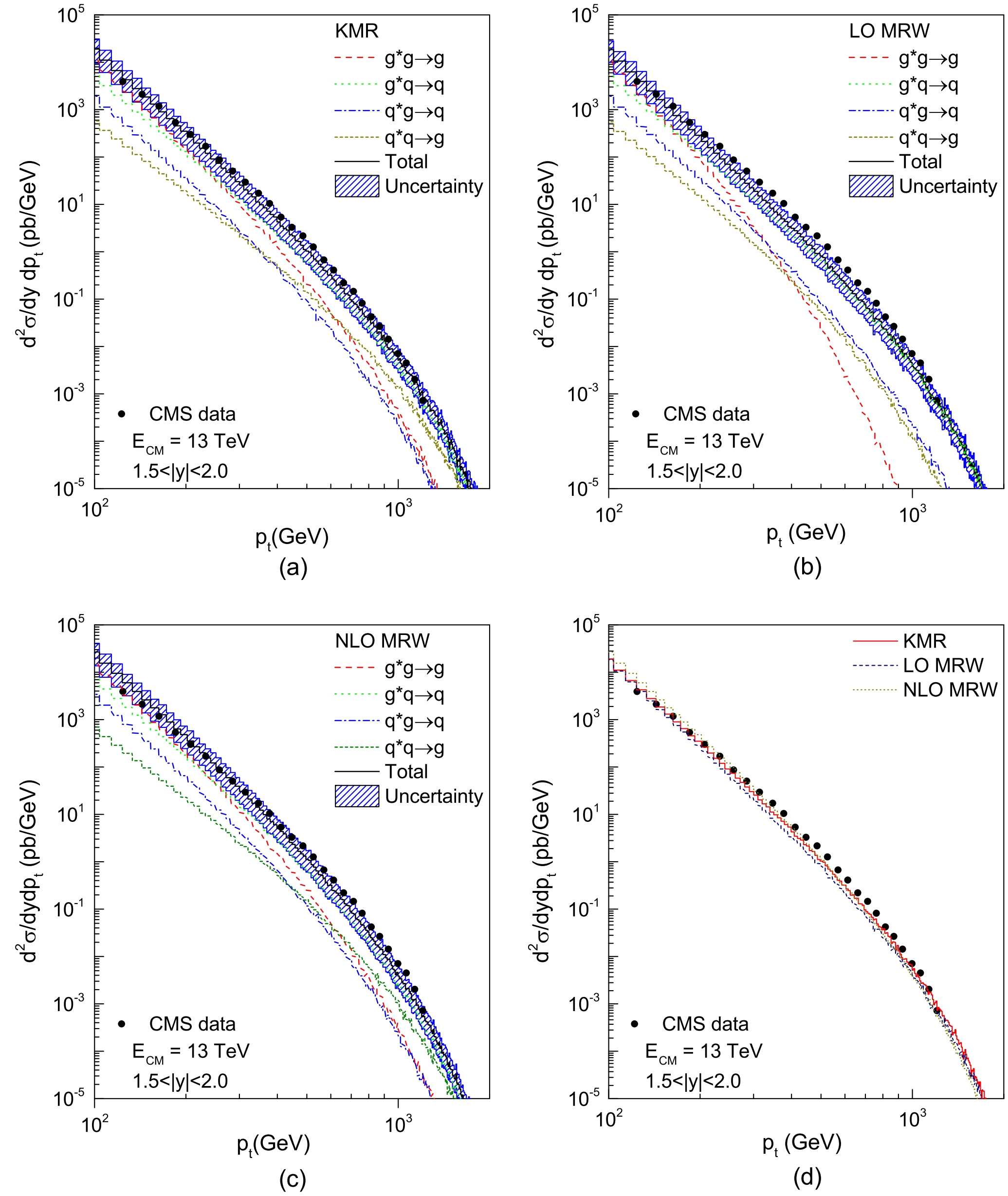

FIG. 11. As Fig. 8 but for a different rapidity region.

In the above equations, k and q are the momentum of the off-shell and the on-shell partons, respectively. k_t is the transverse momentum of the off-shell incoming parton, g_s is the strong coupling, and also C_A and C_f are the color factors for the quark and the gluon, respectively.

Note that the integration boundaries for dk_t^{jet} is $(0, \infty)$, so one can choose an upper limit for these integrations, say $k_{i,\max}$, several times larger than the scale μ. In addition, $k_{t,\min} = \mu_0 \sim 1$ GeV is considered as the lower limit that separates the nonperturbative and the perturbative regions, by assuming that

$$\frac{1}{k_t^2} f_a(x, k_t^2, \mu^2)|_{k_t<\mu_0} = \frac{1}{\mu_0^2} a(x, \mu_0^2) T_a(\mu_0^2, \mu^2). \quad (20)$$

As a result of the above formulation, the density of patrons are constant for $k_t < \mu_0$ at fixed x and μ [36]. For the above calculations, we use the LO-MMHT2014 PDF libraries for the KMR and the LO-MRW UPDF schemes, and the NLO-MMHT2014 PDF libraries for the NLO-MRW formalism [62]. The VEGAS algorithm is considered for performing the multidimensional integration of the cross section in Eq. (8).

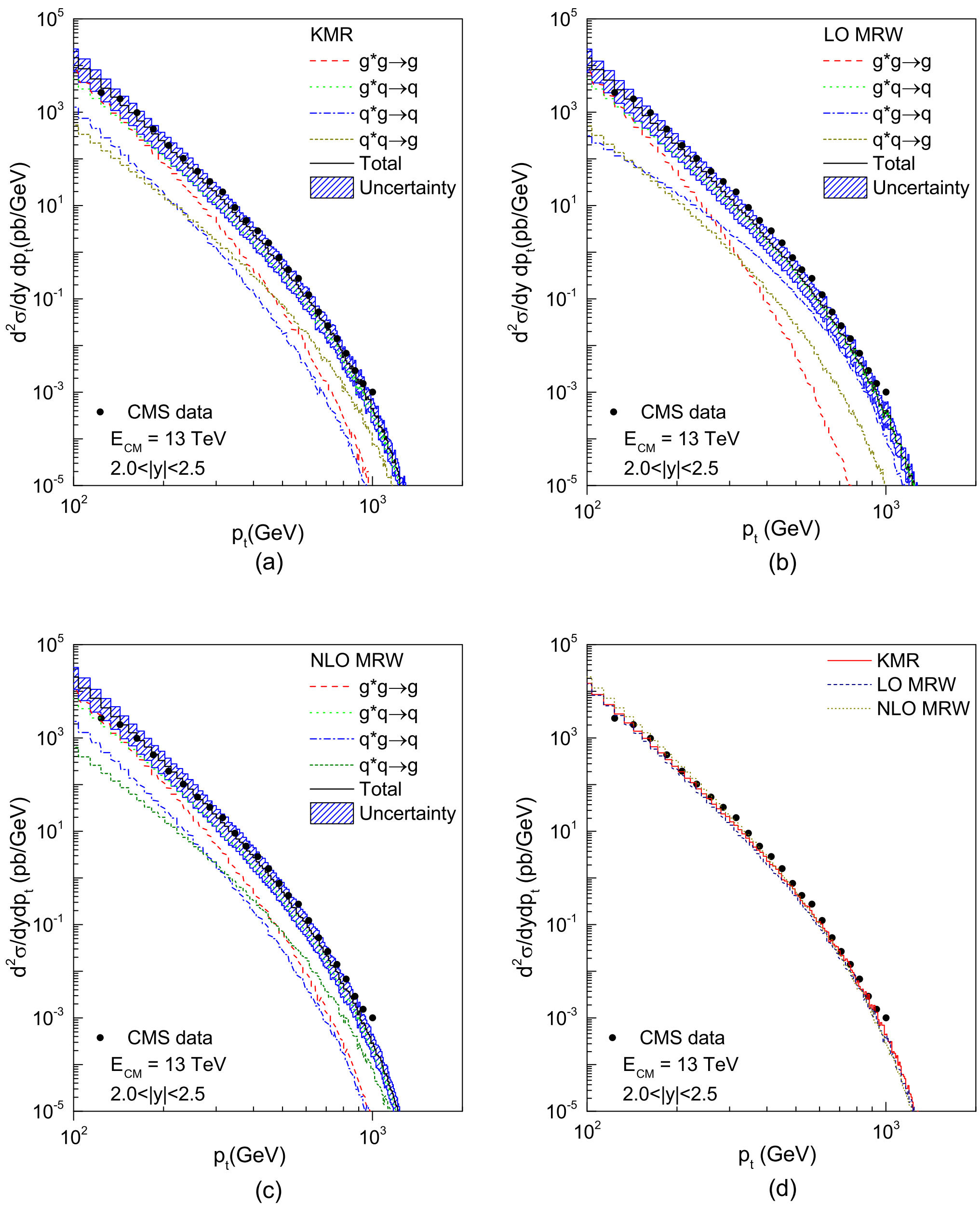

FIG. 12. As Fig. 8 but for a different rapidity region.

III. RESULTS AND DISCUSSIONS

We perform a set of numerical calculations for the production of the single jet at the LHC, using Eq. (8), within the k_t-factorization framework. The results are separated into seven distinct rapidity regions for each center-of-mass energy, in accordance with the specifications of the existing experimental results, i.e., the data from the CMS Collaboration [3,13]. In the following, we intend to present our results, comparisons, and discussions.

In Figs. 1–7, the reader is presented with the double-differential cross section for the production of the single jet ($d^2\sigma/dp_t dy$) as a function of the transverse momentum of the resulting jet (p_t) for $E_{\mathrm{CM}} = 8$ TeV. The corresponding numerical calculations are carried out within the following rapidity regions:

(i) $|y| < 0.5$,
(ii) $0.5 < |y| < 1.0$,
(iii) $1.0 < |y| < 1.5$,
(iv) $1.5 < |y| < 2.0$,
(v) $2.0 < |y| < 2.5$,
(vi) $2.5 < |y| < 3.0$,
(vii) $3.2 < |y| < 4.7$,

which are plotted in Figs. 1–7, respectively. Within each of these figures, panel (a) illustrates the results from the utilization of the KMR UPDF, while panels (b) and (c) show

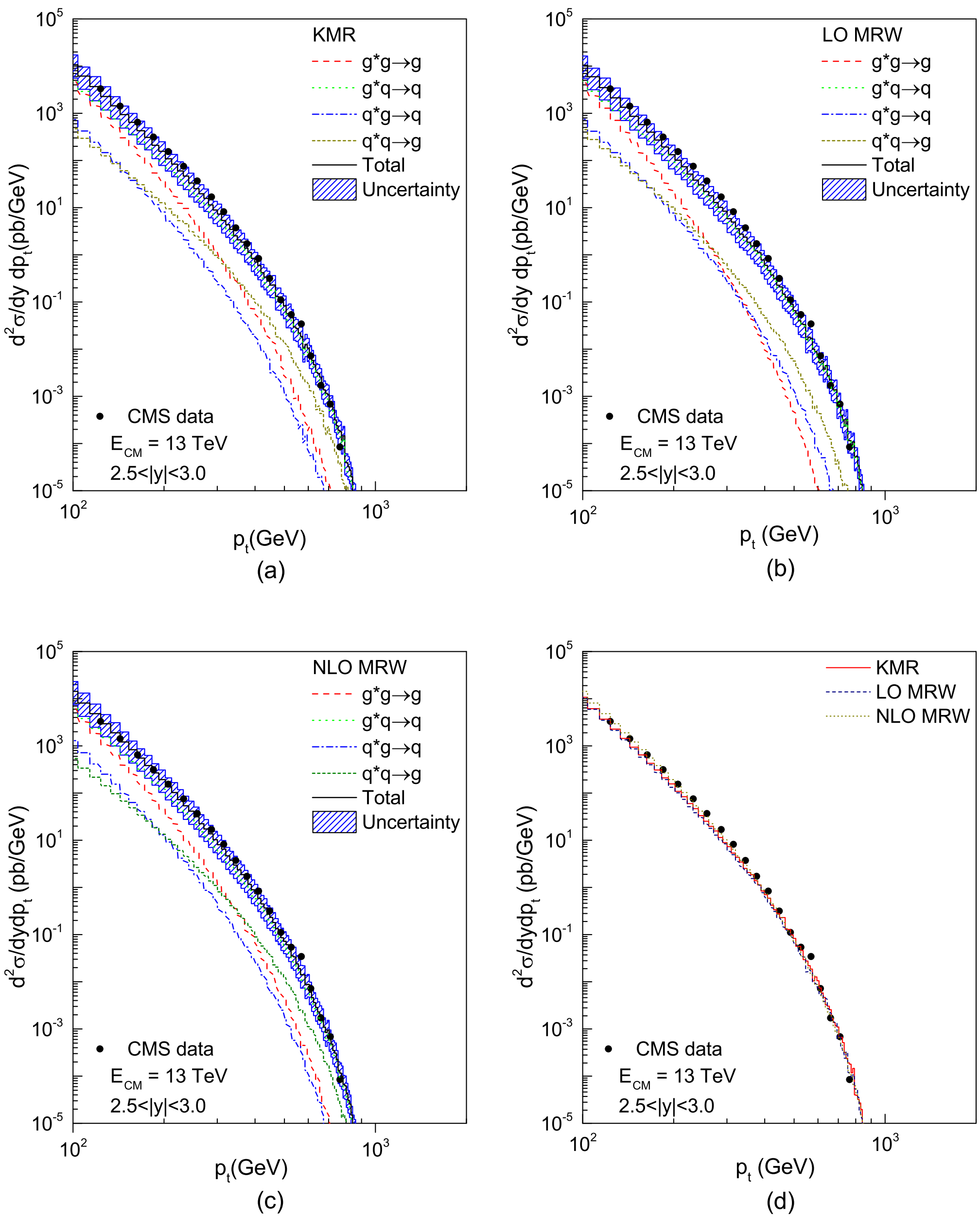

FIG. 13. As Fig. 8 but for a different rapidity region.

the results of the LO and the NLO MRW UPDF, respectively. In each of these panels, the contributions from the partonic subprocesses are demonstrated as follows: $g^* + g \to g$ (the red dashed histograms), $g^* + q \to q$ (the green dotted histograms), $q^* + g \to q$ (the blue dot-dashed histograms), and $q^* + q \to g$ (the olive short-dashed histograms). The sum of these contributions in the respective frameworks are shown with the black solid histograms. The corresponding uncertainty regions (the blue hatched areas) are calculated by manipulating the hard scale μ by a factor of 2.

Having a close look at the contributions from the partonic subprocesses [say at panel (a) of Fig. 1], an interesting dynamic can be observed. At smaller values of the transverse momentum, i.e., $p_t < 100$ GeV, one can clearly see that the $g^* + g \to g$ subprocess has the dominant contribution into the total result:

$$p_t < 100\ \text{GeV}:\ \hat{\sigma}(g^* + g \to g) \gg \hat{\sigma}(g^* + q \to q) > \hat{\sigma}(q^* + g \to q) \gg \hat{\sigma}(q^* + q \to g). \tag{21}$$

Interestingly, the relation (21) does not hold for mid p_t ($100\,\text{GeV} < p_t < 1000\,\text{GeV}$) or high p_t ($p_t > 1000$ GeV) regions. For these later p_t regions, the correlation between the behaviors of the subprocess becomes increasingly framework dependent, showing the deeply intrinsic differences between the used UPDF preparation schemes.

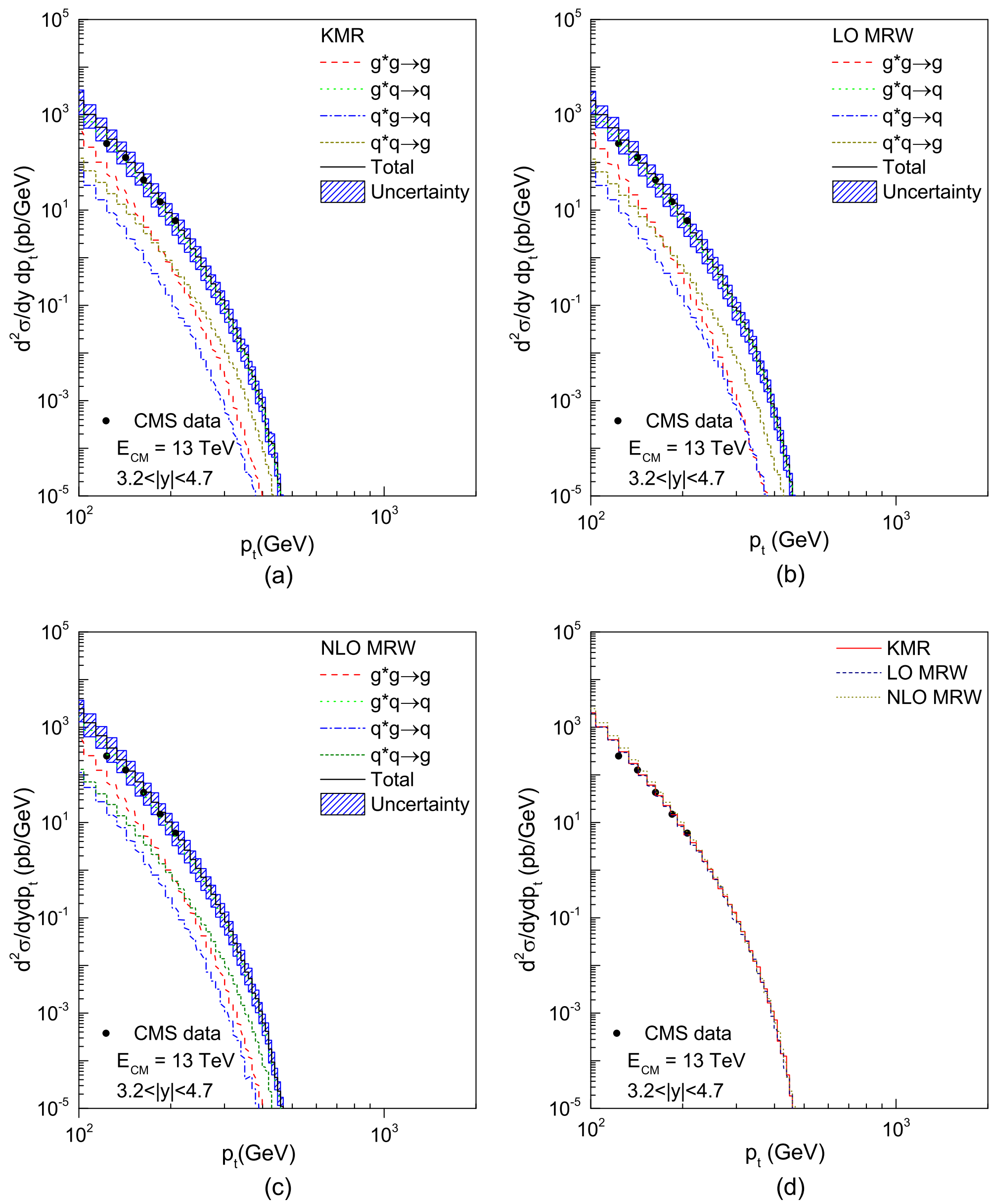

FIG. 14. As Fig. 8 but for a different rapidity region.

Another comparison can be made by moving up between the rapidity regions. It is evident that by increasing the rapidity, clearly the total production rate of the single jet, especially in higher p_t factions, decreases. On the other hand, the calculations that are performed in the k_t-factorization framework tend to maintain (and even slightly increase) their precision in describing the existing experimental data [3].

A comparison between the total contributions are made in panel (d) of the above figures. Despite differences in the behaviors of the partonic subprocesses, these results are relatively similar and are in agreement with the experimental findings. This can be directly credited to the efficiently defined UPDF of the k_t factorization that reliably reduces to the DGLAP PDF at large and moderate values of x. At small-x regions, such as $3.2 < |y| < 4.7$, the dominant factor in determining the behavior of the UPDF would be the constraints on the soft gluon singularities, i.e., the angular ordering constraint. Here, the success of the KMR framework in describing the small-x data is as a result of the effective angular ordering constraint that is inserted on both diagonal and nondiagonal parton emissions at the top of the partonic evolution ladder. So as we have pointed out in our previous works, the resulting differential calculations in contrast to the LO-MRW have similar behaviors in case of KMR and NLO-MRW.

A similar set of calculations are also made for $E_{\mathrm{CM}} = 13$ TeV, corresponding to the experimental data of [13]. The results are presented in Figs. 8–14. Here, the general behaviors of the rapidity regions of the contributing subprocesses are similar to the 8 TeV case. As expected, with increasing the center-of-mass energy of the hadronic collision, the results from the KMR framework maintain their relative success in describing the data. On the other hand, a small decrease in the precision of the LO and NLO MRW predictions can be observed with respect to that of KMR. This can again be contributed to the rise of a higher order contribution at higher E_{CM} and the efficiency of the effective angular ordering constraint in the KMR scheme.

IV. CONCLUSION

Throughout this work, we calculated the production rate of the single-jet events at the LHC for the center-of-mass energies of 8 and 13 TeV, using a simplistic set of LO matrix elements and the UPDF of k_t factorization, i.e., the KMR and the LO and NLO MRW frameworks. We compared our numerical results versus each other and against the experimental data of the CMS Collaboration. Our aim was to illustrate the capability of the above UPDF, which can generally describe the experimental measurements, and not to prove the better precision of such predictions, especially compared to well developed collinear frameworks that are currently being used by different collaborations [47]. We demonstrated that despite the application of the simplistic model, the UPDF of k_t factorization are able to successfully describe the experimental measurements. A further increase in the precision of our calculations is achievable by increasing the higher-order and radiation corrections into the matrix elements as well as providing more accurate UPDF via undergoing a complete phenomenological global fit to the existing deep inelastic data. It was shown that the KMR UPDF cross sections have better agreement to data. On the other hand, they are very similar to those of NLO MRW.

ACKNOWLEDGMENTS

The authors are thankful to Dr. K. Kutak and Dr. A. Lipatov for useful discussions through the preparations of this work. M. M. acknowledges the Research Council of University of Tehran and the Institute for Research and Planning in Higher Education for the grants provided for him.

[1] D. Stump, J. Huston, J. Pumplin, W.-K. Tung, H. L. Lai, S. Kuhlmann, and J. F. Owens, J. High Energy Phys. 10 (2003) 046.
[2] D. Britzger, K. Rabbertz, D. Savoiu, G. Sieber, and M. Wobisch, arXiv:1712.00480.
[3] CMS Collaboration, J. High Energy Phys. 03 (2017) 156.
[4] ATLAS Collaboration, Eur. Phys. J. C **73**, 2509 (2013).
[5] CMS Collaboration, Eur. Phys. J. C **76**, 265 (2016).
[6] ATLAS Collaboration, Eur. Phys. J. C **71**, 1512 (2011).
[7] CMS Collaboration, Phys. Rev. Lett. **107**, 132001 (2011).
[8] ATLAS Collaboration, Phys. Rev. D **86**, 014022 (2012).
[9] CMS Collaboration, Phys. Rev. D **87**, 112002 (2013).
[10] CDF Collaboration, Phys. Rev. D **75**, 092006 (2007).
[11] D0 Collaboration, Phys. Rev. Lett. **101**, 062001 (2008).
[12] CDF Collaboration, Phys. Rev. D **78**, 052006 (2008).
[13] CMS Collaboration, Eur. Phys. J. C **76**, 451 (2016).
[14] V. N. Gribov and L. N. Lipatov, Yad. Fiz. **15**, 781 (1972).
[15] L. N. Lipatov, Sov. J. Nucl. Phys. **20**, 94 (1975).
[16] G. Altarelli and G. Parisi, Nucl. Phys. **B126**, 298 (1977).
[17] Y. L. Dokshitzer, Sov. Phys. JETP **46**, 641 (1977).
[18] A. V. Lipatov, J. High Energy Phys. 02 (2013) 009.
[19] G. Watt, A. D. Martin, and M. G. Ryskin, Phys. Rev. D **70**, 014012 (2004).
[20] G. Watt, Ph.D. thesis, University of Durham, UK, 2004.
[21] S. Baranov, A. Lipatov, and N. Zotov, Phys. Rev. D **81**, 094034 (2010).

[22] A. Lipatov and N. Zotov, Phys. Rev. D **81**, 094027 (2010).
[23] M. Ciafaloni, Nucl. Phys. **B296**, 49 (1988).
[24] S. Catani, F. Fiorani, and G. Marchesini, Phys. Lett. B **234**, 339 (1990).
[25] S. Catani, F. Fiorani, and G. Marchesini, Nucl. Phys. **B336**, 18 (1990).
[26] M. G. Marchesini, in *Proceedings of the Workshop QCD at 200 TeV Erice, Italy*, edited by L. Cifarelli and Yu. L. Dokshitzer (Plenum, New York, 1992), p. 183.
[27] G. Marchesini, Nucl. Phys. **B445**, 49 (1995).
[28] F. Hautmann, M. Hentschinski, and H. Jung, arXiv: 1207.6420.
[29] F. Hautmann, H. Jung, and S. Taheri Monfared, arXiv: 1207.6420.
[30] V. S. Fadin, E. A. Kuraev, and L. N. Lipatov, Phys. Lett. **60B**, 50 (1975).
[31] L. N. Lipatov, Sov. J. Nucl. Phys. **23**, 642 (1976).
[32] E. A. Kuraev, L. N. Lipatov, and V. S. Fadin, Sov. Phys. JETP **44**, 45 (1976).
[33] E. A. Kuraev, L. N. Lipatov, and V. S. Fadin, Sov. Phys. JETP **45**, 199 (1977).
[34] Ya. Ya. Balitsky and L. N. Lipatov, Sov. J. Nucl. Phys. **28**, 822 (1978).
[35] M. A. Kimber, A. D. Martin, and M. G. Ryskin, Phys. Rev. D **63**, 114027 (2001).
[36] A. D. Martin, M. G. Ryskin, and G. Watt, Eur. Phys. J. C **66**, 163 (2010).
[37] M. Modarres and H. Hosseinkhani, Nucl. Phys. **A815**, 40 (2009).
[38] M. Modarres and H. Hosseinkhani, Few-Body Syst. **47**, 237 (2010).
[39] H. Hosseinkhani and M. Modarres, Phys. Lett. B **694**, 355 (2011).
[40] H. Hosseinkhani and M. Modarres, Phys. Lett. B **708**, 75 (2012).
[41] M. Modarres, H. Hosseinkhani, and N. Olanj, Nucl. Phys. **A902**, 21 (2013).
[42] M. Modarres, H. Hosseinkhani, and N. Olanj, Phys. Rev. D **89**, 034015 (2014).
[43] M. Modarres, H. Hosseinkhani, N. Olanj, and M. R. Masouminia, Eur. Phys. J. C **75**, 556 (2015).
[44] M. Modarres, M. R. Masouminia, H. Hosseinkhani, and N. Olanj, Nucl. Phys. **A945**, 168 (2016).
[45] M. Modarres, M. R. Masouminia, R. Aminzadeh Nik, H. Hosseinkhani, and N. Olanj, Phys. Rev. D **94**, 074035 (2016).
[46] M. Modarres, M. R. Masouminia, R. Aminzadeh Nik, H. Hosseinkhani, and N. Olanj, Phys. Lett. B **772**, 534 (2017).
[47] M. Modarres, M. R. Masouminia, R. Aminzadeh Nik, H. Hosseinkhani, and N. Olanj, Nucl. Phys. **B922**, 94 (2017).
[48] M. Modarres, M. R. Masouminia, R. Aminzadeh Nik, H. Hosseinkhani, and N. Olanj, Nucl. Phys. **B926**, 406 (2018).
[49] M. Bury, M. Deak, K. Kutak, and S. Sapeta, Phys. Lett. B **760**, 594 (2016).
[50] P. Kotko, K. Kutak, C. Marquet, E. Petreska, S. Sapeta, and A. van Hameren, J. High Energy Phys. 09 (2015) 106.
[51] K. Kutak and J. Kwiecinski, Eur. Phys. J. C **29**, 521 (2003).
[52] K. Kutak and A. M. Stasto, Eur. Phys. J. C **41**, 343 (2005).
[53] K. Kutak and S. Sapeta, Phys. Rev. D **86**, 094043 (2012).
[54] J. Kwiecinski, A. D. Martin, and A. M. Stasto, Phys. Rev. D **56**, 3991 (1997).
[55] K. Kutak, Phys. Rev. D **91**, 034021 (2015).
[56] K. Kutak, R. Maciula, M. Serino, A. Szczurek, and A. van Hameren, J. High Energy Phys. 04 (2016) 175.
[57] A. Dumitru, A. Hayashigaki, and J. Jalilian-Marian, Nucl. Phys. **A765**, 464 (2006).
[58] M. Deak, Ph. D. thesis, University of Hamburg, Germany, 2009.
[59] J. Collins, *Foundation of Perturbative QCD* (Cambridge University Press, Cambridge, UK, 2011).
[60] K. Golec-Biernat and A. M. Stasto, arXiv:1803.06246v1.
[61] M. A. Kimber, A. D. Martin, and M. G. Ryskin, Eur. Phys. J. C **12**, 655 (2000).
[62] L. A. Harland-langg, A. D. Martin, P. Motylinski, and R. S. Thorne, Eur. Phys. J. C **75**, 204 (2015).